Untargeted Profiling of Concordant/Discordant Phenotypes of High Insulin Resistance and Obesity To Predict the Risk of Developing Diabetes

Anna Marco-Ramell,[†,§] Sara Tulipani,[†,¶] Magali Palau-Rodriguez,[†,§] Raul Gonzalez-Dominguez,[†,§]Antonio Miñarro,[‡] Olga Jauregui,[†,∥] Alex Sanchez-Pla,[‡,#] Manuel Macias-Gonzalez,[¶,⊥] Fernando Cardona,[¶,⊥] Francisco J. Tinahones,[¶,⊥] and Cristina Andres-Lacueva[*,†]

†Biomarkers & Nutrimetabolomics Laboratory, Nutrition and Food Science Department, Food Technology Reference Net (XaRTA), Nutrition and Food Safety Research Institute (INSA-UB), Faculty of Pharmacy and Food Sciences, Pharmacy and Food Science Faculty and ‡Genetics, Microbiology and Statistics Department, Biology Faculty, University of Barcelona, Barcelona 08028, Spain

§CIBER Fragilidad y Envejecimiento Saludable [CIBERfes] and ⊥CIBER Fisiopatología de la Obesidad y Nutrición [CIBERobn], Instituto de Salud Carlos III [ISCIII], Madrid 28029, Spain

¶Biomedical Research Institute [IBIMA], Service of Endocrinology and Nutrition, Malaga Hospital Complex [Virgen de la Victoria], Campus de Teatinos s/n, Malaga 29010, Spain

∥Scientific and Technological Centres of the University of Barcelona (CCIT-UB), Barcelona 08028, Spain

#Statistics and Bioinformatics Unit, Vall d'Hebron Institut de Recerca [VHIR], Barcelona 08035, Spain

ABSTRACT

This study explores the metabolic profiles of concordant/discordant phenotypes of high insulin resistance (IR) and obesity. Through untargeted metabolomics (LC-ESI-QTOF-MS), we analyzed the fasting serum of subjects with high IR and/or obesity (n = 64). An partial least-squares discriminant analysis with orthogonal signal correction followed by univariate statistics and enrichment analysis allowed exploration of these metabolic profiles. A multivariate regression method (LASSO) was used for variable selection and a predictive biomarker model to identify subjects with high IR regardless of obesity was built. Adrenic acid and a dyglyceride (DG) were shared by high IR and obesity. Uric and margaric acids, 14 DGs, ketocholesterol, and hydroxycorticosterone were unique to high IR, while arachidonic, hydroxyeicosatetraenoic (HETE), palmitoleic, triHETE, and glycocholic acids, HETE lactone, leukotriene B4, and two glutamyl-peptides to obesity. DGs and adrenic acid differed in concordant/discordant phenotypes, thereby revealing protective mechanisms against high IR also in obesity. A biomarker model formed by DGs, uric and adrenic acids presented a high predictive power to identify subjects with high IR [AUC 80.1% (68.9− 91.4)]. These findings could become relevant for diabetes risk detection and unveil new potential targets in therapeutic treatments of IR, diabetes, and obesity. An independent validated cohort is needed to confirm these results.

KEYWORDS: adrenic acid, diglycerides, insulin resistance, metabolic profiles, metabolomics, obesity, observational study, predictive model, ROC curves, uric acid

1. INTRODUCTION

Metabolic disorders such as insulin resistance (IR) and obesity are major health problems. IR plays an important pathophysiological role in the development of diabetes and metabolic syndrome. Obesity is also usually accompanied by other metabolic comorbidities such as IR, diabetes, and cardiovascular complications.1,2 Nevertheless, not all the subjects with obesity develop IR or diabetes, and individuals with IR are not always overweight. Subjects with obesity can be insulin-sensitive (IS) and have normal blood pressure and lipid profiles, whereas normal weight individuals

can present IR and β-cell impairment. 3,4 The inclusion of discordant phenotypes in research studies has shed light on new insights into the metabolic processes uniquely related to obesity or diabetes, and therefore dug more deeply into the interrelation between obesity and the development of diabetes.5 Metabolomics is the high-throughput technology that explore the global metabolic state (metabolome) of an individual by analyzing the low-molecular-weight compounds (metabolites) within a biological sample.6 Over the past decade, metabolomics has been used to identify predictive and prognostic biomarkers and to monitor the efficacy of treatments.7,8 Moreover, metabolomics has also been employed to uncover the molecular processes involved in pathophysiological states and to describe individual metabolic phenotypes (metabotypes), which can be exploited in personalized medicine and public healthcare.9 Untargeted metabolomics is a promising tool for elucidating novel mechanisms and finding disease biomarkers. It measures hundreds of metabolites and can detect previously unpredicted metabolic perturbations associated with a certain disease.6 Few untargeted metabolomic studies have explored the metabolic profiles of diabetes and obesity, and very few of high IR regardless of obesity. The comprehensive analysis of the metabolome of subjects with high IR could be key in discovering a new gold standard to predict the progression of IR and the risk of developing diabetes. The aims of this work are three-fold: (1) to explore the metabolic profiles of high IR and obesity; (2) to identify differences between concordant/discordant phenotypes of high IR and obesity; and (3) to define a predictive model for the risk of developing of diabetes. To these ends, we have carried out an untargeted metabolomic approach on fasting serum of human concordant/discordant phenotypes of high IR and obesity, followed by multivariate and univariate statistics, and an enrichment analysis. Finally we have built different predictive models of combined serum markers to identify subjects with high IR through a multivariate logistic regression and assessed their performance with ROC curves.

■ MATERIALS AND METHODS

Subjects and Study Design

Sixty-four adult individuals (19 men and 45 women) were recruited at the Virgen de la Victoria University Hospital and Carlos Haya Hospital (Malaga, Spain). A detailed description of the study design and inclusion/exclusion criteria has been previously reported.5 Individuals were classified according to (1) the risk of developing diabetes type 2, based on fasting plasma glucose (FG) and the Homeostatic Model Assessment-Insulin Resistance index (HOMA-IR), in low IR or IS if FG < 100 mg/dL and HOMA-IR < 2.5, or high IR if 100 ≤ FG < 126 mg/dL and HOMA-IR > 3.4; and (2) body mass index (BMI), in nonobesity if 18.5 < BMI ≤ 26.9 kg/m2 or subjects with obesity if BMI > 40 kg/m2. The FG cutoff was defined by the American Diabetes Association,10 and the HOMA-IR cutoff was obtained experimentally.5 Subsequently, four sex-matched phenotypic groups were obtained as follows: subjects with (1) IS and nonobesity (control group, n = 19); (2) IS and obesity (n = 12); (3) high IR and non-obesity (n = 12); and (4) high IR and obesity (n = 21). The protocol was approved by the local Ethics and Research Committees (Hospital Universitario Virgen de la Victoria, Malaga) and all participants provided written informed consent.

Anthropometric and Biochemical Parameters

The following anthropometric and biochemical parameters were measured, as previously described:5 (1) adiposity markers (body weight (kg), BMI (kg/m2), waist and hip circumference (cm) and waist-hip ratio); (2) IR markers (FG (mmol/L), fasting insulin (μU/mL), HOMA-IR index); (3) blood pressure (diastolic and systolic blood pressure (mm Hg)); and (4) lipid markers (total cholesterol, low-density lipoprotein (LDL) and high-density lipoprotein (HDL) cholesterol, and triglycerides (TG), mmol/L).

Reagents

Acetylcholine, acetyl-d3-L-carnitine hydrochloride, acetyl-Lcarnitine, adrenic acid, L-carnitine, L-citrulline, dodecanoic acid, (−)-epicatechin, gallic acid, glycochenodeoxycholic acid, glycocholic acid, glycocholic acid-(glycyl-1−13C) monohydrate, α-hydroxyisobutyric acid, indole-3-acetic-2,2-d2 acid, Lisoleucine, 7-ketocholesterol, L-leucine, leukotriene B4, margaric acid, palmitic acid, L-phenylalanine, stearic acid, syringic acid, L-tryptophan, uric acid, and L-valine were purchased from

Sigma-Aldrich (St. Louis, MO). 4-hydroxyhippuric acid was purchased from PhytoLab GmbH and Co KG (Vestenbergsgreuth, Germany), naringenin from Extrasynthèse (Genay, France), and arachidonic acid from Cymit Quimica (Barcelona, Spain). UHPLC−MS-grade methanol, acetone, formic acid, and HPLC-grade acetonitrile were purchased from Scharlau Chemie S.A. (Barcelona, Spain). Ultrapure water (Milli-Q) was obtained from a Milli-Q Gradient A10 system (Millipore, Bedford, MA).

Quality Controls and Standards

An aqueous mix of metabolite standards (quality control, QC) and internal/external standards was prepared, as previously described,11 to monitor instrumental stability. Water was used as QC1. A mix of standards (QC2) containing acetylcholine, acetyl-d3-L-carnitine hydrochloride, acetyl-L-carnitine, L-carnitine, L-citrulline, dodecanoic acid, (−)-epicatechin, gallic acid, glycochenodeoxycholic acid, glycocholic acid-(glycyl-1−13C) monohydrate, α-hydroxyisobutyric acid, indole-3-acetic-2,2-d2 acid, L-isoleucine, L-leucine, palmitic acid, L-phenylalanine, stearic acid, syringic acid, L-tryptophan and L-valine, spiked in Milli-Q water and plasma, was prepared (5 ppm final concentration). Finally, a 10% of the samples, randomly selected, were reanalyzed to assess differences between replicates (QC3). Aqueous solutions of isotopically labeled and unlabeled compounds were also prepared and used during sample extraction. A mixture of glycocholic acid-(glycyl-1−13C) monohydrate and 1-O-stearoyl-sn-glycero-3-phosphocholine (25 ppm final concentration) was used as internal standard, and a mixture of indole-3-acetic-2,2-d2 acid and acetyl-d3-Lcarnitine hydrochloride (25 ppm final concentration) as external standard. Adrenic acid, arachidonic acid, glycocholic acid, 7-ketocholesterol, leukotriene B4, margaric acid, palmitoleic acid, and uric acid (50 ppb ppm final concentration) were spiked in Milli-Q water and plasma to confirm the identity of annotated metabolites.

Sample Treatment and Data Acquisition

Fasting serum samples (50 μL) were subjected to in-plate hybrid extraction, previously optimized by Tulipani et al. Samples were first deproteinized by acidic solvent precipitation (acetonitrile in 1%

formic acid), followed by phospholipid solid phase extraction (SPE)-mediated removal.12 A TripleTOF 6600 hybrid quadrupole-TOF mass spectrometer (AB Sciex, Framingham, MA) with Turbo Spray IonDrive source coupled to a Shimadzu Nexera X2 series HPLC system (Kyoto, Japan) (Atlantis T3 RP column 50 × 2.1 mm2, 5 μm (Waters, Milford, MA)) was used. A linear gradient elution was used ([A] Milli-Q water 0.1% HCOOH (v/v) and [B] methanol (v/v)), at a constant flow rate of 600 μL min−1 as follows (time, min; B, %): (0, 1), (4, 20), (6, 95), (7.5, 95), (8, 1), (12, 1). Data acquisition was performed by liquid chromatography−mass spectrometry (LC−MS) from 70 to 850 m/z with positive and negative electrospray ionization (ESI + and ESI−). The sample injections order was randomized to avoid bias. QC samples were analyzed throughout the run every 15 injections to provide measurements of the stability and performance of the system and evaluate the quality of the data.12,13 Calibration was carried out with calibration solutions for AB Sciex TripleTOF systems (AB Sciex) in ESI+ and ESI− modes. The mass spectrometry data have been deposited to the MetaboLights repository14 (https://www.ebi.ac.uk/ metabolights/) with the data set identifier MTBLS668.

Data Preprocessing

LC−MS data were preprocessed with MarkerView 1.3.0.1 (AB Sciex) (Tables S1 and S2). Raw data contained 3000 mass features, including redundant mass signals (isotopes, adducts, in-source fragments, etc.). The data sets were filtered out to remove variables that did not appear in more than 25% of any of the groups.11 The final data sets presented 2607 (ESI+) and 2318 (ESI−) mass features. ESI+ and ESI− data sets were analyzed separately.

Multivariate Statistical Analysis

Partial least-squares discriminant analysis with orthogonal signal correction (OSC-PLS-DA) was used to examine between-group differences in LC−MS data (SIMCA-P+ 13.0 software, Umetrics, Umeå, Sweden). Data were log-transformed and Pareto scaled,15,16 and an OSC filter was applied to remove the variability not associated with the diseases. Comparisons were performed by comparing the control group (IS and nonobesity, n = 19) with the high IR group (subjects with high

IR (non-obesity + obesity), n = 33) or the obesity group (subjects with obesity (IS + high IR), n = 33). The robustness of the models was evaluated through the R2X (cum), R2Y (cum), and Q2 (cum) parameters, cross-validation and permutation tests (n = 200) (Table S3). As a final quality test, the data set was randomly split into ten equal-size subsamples, nine of which were used as a training set while the remaining was used as a validation set. This process was repeated ten times (Table S4). Mass features explaining group separation were selected according to their variable importance for projection (VIP) values (cutoff ≥ 2).

Annotation of Metabolites

A cluster analysis, based on Pearson correlation and Ward's distance method,17 was used to determine eventual clusters of mass features from the same metabolite (PermutMatrix 1.9.3). MetaNetter, a plugin for Cytoscape (v.2.8.0), was used to define adducts and fragments within the cluster.18 The annotation of metabolites was carried out by comparing MS and MS/MS experimental data with in-house (MAIT19) and online databases including HMDB, METLIN, LipidMAPS, MassBank and MetFrag (±5 mDa mass error tolerance). The fragmentation of [M+H]+ and [M+Na]+ ions enabled the characterization of fatty acids contained in the glycerolipid structure. The fatty acid composition of diglycerides (DG) was annotated based on characteristic daughter ions in the m/z range 200−400 Da, generated through the release of fatty acids from the glycerol backbone.20 Metabolite identity confirmation was carried out by matching peak chromatographic and MS responses (extracted ion chromatogram, product ion scan) to those of commercial reference standards, when available, spiked in Milli-Q water and plasma (50 ppb), on a QStar Elite system (AB Sciex). The analytical parameters were the same as described above.

Univariate Statistical Analysis

Univariate analysis was performed in R to describe differences in clinical and metabolic parameters. Clinical parameters were first log-transformed prior to the analysis. Statistics on metabolic parameters were performed on the raw matrix. Prior to the analyses, data were log-normalized and Pareto scaled. A type III ANOVA for unbalanced groups was performed to assess the effects of

obesity and high IR on clinical variables. Fisher's exact test was used to evaluate differences in gender distribution across the groups.21 A Student's t test was used to confirm that the metabolites with a VIP ≥ 2 differed between groups, and to identify differences between concordant and discordant phenotypes of each metabolic disorder. All p-values were corrected by false discovery rate (FDR) to reduce the probability of false positives.22 Gender, age and drug consumption were considered as confounders in all the analyses. Only those metabolites with adjusted p-value ≤ 0.05 were considered significant.

Enrichment Analysis

ChemRICH (http://chemrich.fiehnlab.ucdavis.edu/) was used to perform an enrichment analysis of the metabolites that presented VIP ≥ 2 and adjusted p-value ≤ 0.05. ChemRICH utilizes structure similarity and chemical ontologies to map all known metabolites and name metabolic modules. The ChemRICH statistical approach compares chemical similarities using the Medial Subject Headings database and Tanimoto chemical similarity coefficients to cluster metabolites into nonoverlapping chemical groups. Enrichment statistical analysis uses a background-independent database test, Kolmogorov− Smirnov-test, using the created clusters.23

Predictive Models of Combined Serum Markers

Variable selection was performed with all the metabolites that met both criteria, VIP ≥ 2 and adjusted p-value ≤ 0.05, for high IR to select those compounds that better separate subjects with IS or high IR. A new metabolic variable, total diglycerides (tDG), was created with the arithmetic mean of all DGs. Variable selection was conducted with the least absolute shrinkage and selection operator (LASSO) logistic regression using a leave-one-out cross-validation.24 Prior to the analysis, data were log-normalized and Pareto scaled, and adjusted by gender, age, and drug consumption. The lambda-coefficient was used to choose the most predictive metabolites, and these were employed to build a new parameter, the multimetabolite biomarker model, as follows: Multimetabolite biomarker model = λ1 X metabolite 1 + λs X metabolite 2 + …. + λn X metabolite n The LASSO regression method was performed in R with the glmnet package.

ROC Curves

The global performance of this multimetabolite biomarker model was evaluated through receiver operating characteristic (ROC) curves. The area under the curve (AUC) value, confidence intervals (CIs 95%), sensitivity, and specificity were calculated in R with the pROC package.

RESULTS

Anthropometric and Biochemical Parameters

Individuals with high IR presented altered FG, fasting insulin, HOMA-IR index, and lipid metabolism indicators (total cholesterol, HDL, and LDL cholesterol and TG). Subjects with obesity had higher adiposity markers, systolic and diastolic pressure, and total cholesterol than individuals without obesity. No changes were observed in the interaction between high IR and obesity for any of the variables (Table 1). Differences between concordant and discordant phenotypes of high IR were mainly due to adiposity markers. Subjects with concordant and discordant phenotypes of obesity also presented metabolic differences including FG, fasting insulin, HOMA-IR index, and lipid metabolism (Table 1).

LC−MS Data Quality

Neither carryover nor apparent clustering due to the batch injection order were noticed (Figure S1). The run-to-run repeatability of the QCs across the whole data set met the quality criteria (retention time shift ≤ 0.05 min, mass accuracy deviation <3 mDa and peak area CV < 25%)11 (Table S1). The generation of the OSC filters removed six and five components (eigenvalue >2), maintaining the 54% and 76% non-orthogonal variation in the original ESI+ and ESI− data sets, respectively. The OSC-PLS-DA resulted in four robust models that discriminate metabolic differences among control individuals and subjects with high IR or obesity (Figure 1, Table S3). The PLS score plot showed that the control group and the high IR or obesity groups clearly separated in the first component. The plot also suggested that concordant and discordant phenotypes of each disorder (high IR-obesity vs high IR-non-obesity, and IS-non-obesity vs IS-obesity, respectively) might be metabolically different

as they were slightly separated in the second component (Figure 1). A total of 193 (ESI+) and 169 (ESI−) mass features were selected (VIP value ≥ 2) for further metabolite identification(Figure S2).

Metabolic Profiles of High IR and Obesity

A total of 29 metabolites (VIP ≥ 2) were annotated from their m/z value and/or fragmentation pattern, and the identity of eight of them was confirmed with metabolite standards (Table 2). The majority of the metabolites were lipids. We were not able to discern between a molecular ion or sodium adduct in DGs since both species presented a small mass difference with the theoretical mass (<3 mDa). Thus, we provided both annotations. A Student's t test confirmed that two out of these compounds were shared by both metabolic statuses, 18 were only found in high IR and nine in obesity. Adrenic acid and a DG (34:2/36:5) were common between high IR and obesity, which were higher than in the control group. Metabolomics also revealed that the high IR group presented more DGs, margaric acid, ketocholesterol, and uric acid, and lower levels of hydroxycorticosterone. On the other hand, alterations in lipid metabolism were also found in obesity. For instance, the obesity group showed higher levels of arachidonic acid, HETE, HETE lactone, leukotriene B4, palmitoleic acid and tryhydroxyeicosatetraenoic acid (triHETE), and the dipeptides γ- glutamyl-γ-aminobutyraldehide and glutamyl-valine than the control groups, and lower levels of the bile acid glycocholic acid (Figure 2). An enrichment analysis was performed with ChemRICH to identify which chemical class was more enriched in each metabolic disorder. ChemRICH revealed that the most enriched chemical class in high IR was DGs (adjusted p-value = $2.2 \times 10{-}20$), while HETEs and unsaturated fatty acids were in obesity (adjusted p-values = $1.7 \times 10{-}05$ and $6.0 \times 10{-}04$, respectively) (Table 3). Therefore, we will mainly focus the discussion of the results in these chemical classes.

Metabolic Differences between Concordant/Discordant Phenotypic Groups

Comparisons between phenotypic groups confirmed that the main differences between groups were due to DG and polyunsaturated fatty acid (PUFA) levels, revealing that the degree of dyslipidemia and pro-inflammatory markers could differentiate subjects of distinct phenotypic groups (Figure 3).

Among all the PUFAs, adrenic acid was the only metabolite able to distinguish subjects with IS from those with high IR, and individuals with obesity from those without obesity (Table S5).

Predictive Models of Combined Serum Markers

A combined multimetabolite biomarker model to identify individuals with high IR was formed with the arithmetic mean of DGs (tDG), uric acid, and adrenic acid. This model presented a high predictive power. Specifically, the AUC (95% CI) for the multimetabolite biomarker model was 80.1% (68.9−91.4) when analyzing all the population of the study, 72.5% (53.3−91.7) for the subjects with obesity, and 80.7% (61.0−100) for individuals without obesity (Figure 4). Sensitivity and specificity rates were between 70 and 90%. In the case of subjects with obesity, predictive values were slightly lower (Table 4). This predictive model presented better performance than the combination of other lipid markers such as cholesterol or TG between them and/or with uric acid and adrenic acid (Table S6).

DISCUSSION

The untargeted profiling of the serum of concordant/ discordant phenotypes of high IR and/or obesity allowed exploring the metabolic profiles of these two metabolic statuses and describing their similarities and divergences. In addition, it allowed defining a multimetabolite biomarker model to detect high IR regardless of obesity, which might predict the risk developing diabetes. Large disturbances in lipid metabolism were observed in all the metabolic disorders.

Metabolic Profile of High IR

DGs were the most enriched chemical class in subjects with high IR. This group also presented differences in TG levels, whose levels highly correlate with DG levels (Pearson's correlation coefficient: $r = 0.90$). However, TG species could not be detected in metabolomic profiles because of their very low polarity, which provokes that most TGs remain adsorbed into the protein precipitate during serum extraction. Furthermore, these neutral lipids are not readily ionized in ESI, unless some modifier is added to mobile phases (e.g., ammonium salts). Despite the adipocytokines-induced

inflammation is the prevailing hypothesis of IR progression, the hypothesis of DGmediated IR is becoming increasingly important.26,27 In line with this hypothesis, we observed higher levels of DGs in subjects with high IR regardless of obesity. An accumulation of DGs leads to a cascade of events such as the activation of isoforms of protein kinase C that inhibit sensibility to insulin of insulin responsive tissues, the reduction of fatty acid β- oxidation in the mitochondria, thereby limiting energy production, and lipodystrophy in tissues due to the redistribution of fat.26,27 Adrenic acid was the only PUFA whose levels were altered in subjects with high IR, suggesting a certain degree of a proinflammatory response. Adrenic acid is a ω-6 PUFA. This class of lipids act as inflammatory mediators by acting as ligands for immune receptors and trigger a perpetual low-grade inflammation. This low-grade inflammation leads to a cascade of events including inflammatory cell activation, adipocyte growth and dysfunction, oxidative stress and altered signaling.28,29 Uric acid, a product of the metabolic breakdown of purine nucleotides, was also higher in subjects with high IR. It is normally excreted by the urine but high concentrations of uric acid in blood are associated with oxidative stress, inflammation and alterations in carbohydrate and lipid metabolism. For instance, hyperuricemia promotes endothelial cell damage and dysfunction, decreases endothelial nitric oxide availability, which limits insulin action, increases reactive oxygen species, and blocks adiponectin synthesis. In addition, hyperuricemia alters gluconeogenesis, fatty acid oxidation, and induces the production of pro-inflammatory mediators. Serum uric acid has been proposed as a risk marker in IR, cardiovascular disease, metabolic syndrome and renal failure, among others.30,31 The precursor of aldosterone, hydroxycorticosterone, was lower in subjects with high IR. Hypoaldosteronism has been associated with adrenal insufficiency and diabetic nephropathy. 32 Results from the cohort Framingham Heart Study described a lineal relationship between the glycaemic index and the risk for renal alterations, even before the onset of diabetes.33 Therefore, alterations in uric acid and hydroxycorticosterone might reflect that subjects with high IR may be prone to develop renal alterations. Furthermore, higher levels of 7-ketocholesterol might also confirm oxidative processes in high IR. 7-ketocholesterol, also known as 5-cholesten-3β-ol-7-one, is a sterol derived from the oxidation of cholesterol and it has been proposed as a robust biomarker of oxidized LDL particles in

a range metabolic disorders.34 Energy misbalance, hyperglycaemia, and hyperlipidaemia can lead to increase the production of free radicals, which might damage cellular structures and alter metabolic processes.35,36

Metabolic Profile of Obesity

Dyslipidemia was also observed in obesity. For instance, the blood levels of free fatty acids (FFA) such as palmitoleic acid and ω-6 PUFAs were higher in the obesity group than in the control group. In physiological conditions, blood FFA levels are tightly regulated. However, in obesity and other metabolic disorders, FFA increase in plasma due to the stress of the adipose tissue, which releases more FFA than in normal conditions.37 The enrichment analysis with ChemRICH revealed that HETEs and unsaturated fatty acids were the most enriched chemical classes in subjects with obesity. For instance, adrenic acid, arachidonic acid, HETE, HETE lactone, leukotriene B4 (diHETE), and triHETE levels were found to be higher in the obesity group. These metabolites belong to the ω-6 PUFAs class and, as already commented, they are lipid mediators that trigger a perpetual low-grade inflammation. Arachidonic acid is considered the primary source of pro-inflammatory lipid mediators and it is rapidly converted into potent inflammatory mediators such as prostaglandins, thromboxanes, leukotrienes, lipoxins and HETEs, and derivatives, which lead to cascade of events, as described hereinbefore.28,29 Therefore, the fact that we found more ω-6 PUFAs differentially expressed in obesity than in high IR with respect to the control group (Table 2), and their levels were higher in concordant than in discordant phenotypes (Figure 3, Table S5), suggests that the inflammatory processes in high IR might be at a lower extent than in obesity. Inflammation and oxidative stress are tightly interconnected processes. For instance, inflammatory cells produce free radicals during the immune response.35,36 Although 7-ketocholesterol was not altered in obesity, two glutamyl peptides, namely glutamyl-γ-aminobutyraldehyde and glutamyl-valine, levels were higher in obesity. Glutamyl dipeptides, formed by glutamate and another amino acid, are byproducts of glutathione synthesis and their levels are an indirect evidence of glutathione synthesis and amino acid availability.38 γ-aminobutyraldehyde is the direct precursor of γ-aminobutyric acid (GABA). Both

GABA and glutamate stimulate food intake and body weight gain.39 Valine has also been associated with obesity as branched-chain amino acids (BCAAs) fuel adipocytes.40 Glutamate and BCAA levels also correlated with anthropometric adiposity markers in a previous study, probably as an alternative energy source to compensate glucose and lipid metabolism impairment.5 Therefore, higher levels of these dipeptides in obesity might mirror oxidative stress, the stimulation of appetite, body weight gain, and the use of alternative energy sources in the group with obesity. Bile acids are involved in the absorption of dietary fat and fatsoluble vitamins and modulate cholesterol level, but also regulate energy homeostasis and can act as signaling molecules and inhibit obesity. We found lower levels of glycocholic acid, a primary bile acid conjugated with glycine, in obesity. Thus, alterations in this bile acid might reflect body weight, lipid and carbohydrate metabolism alterations in obesity.41 In addition, this decrease of primary bile acids might alter the release of glucagon-like peptide-1 (GLP-1), thus modifying satiety and appetite of individuals with obesity.42 This observation agrees with the higher levels of the dipeptide formed by glutamate and the direct precursor of GABA. Increases in conjugated bile acids have been found in patients with obesity after undergoing bariatric surgery.43

Differences between Concordant/Discordant Phenotypes of High IR and Obesity

The main differences between the four phenotypic groups were DGs and PUFA levels. The highest levels of these metabolites were found in subjects with both high IR and obesity, while the lowest levels in individuals with both IS and non-obesity. In addition, this study also revealed that the metabolic profile of subjects with only one metabolic disorder, high IR or obesity, had lower levels of DGs, free fatty acids and pro-inflammatory markers than individuals presenting both disorders. These results might unveil that obesity itself also implies the existence of protective mechanisms against high IR. In line with this observation, differences in pro-inflammatory markers in subjects with obesity and IS or IR have been already described. This observation is also known as the “obese healthy paradox”.44,45 Among all the metabolites identified as potential markers of discordant phenotypes of high IR and obesity (Table S5), adrenic acid is particularly interesting since it is the only compound whose levels allowed differentiating the four phenotypical groups. Adrenic acid

(C22:4 n-6) is a minor ω- 6 PUFA in blood, it derives from the elongation of arachidonic acid in the liver and its production increases in inflammation.46 However, little literature about its role in healthy conditions is known. Further research on this particular lipid could provide more insights about differences between concordant/discordant phenotypes in metabolic disorders.

Multimetabolite Biomarker Model To Predict Risk of Developing Diabetes

IR sets in before disease markers appear and it might remain undiagnosed for a long period, thereby increasing the risk of developing other metabolic alterations. Therefore, there is a need to detect IR rapidly and to monitor its progression to diabetes. Although current markers have a high predictive power, they also present some limitations.1 Current markers of high IR such as FG, fasting insulin or HOMA-IR presented a high predictive power (not shown, AUC ≈ 95%). It may be because subjects were grouped according their FG levels and HOMA-IR index. However, they may be late markers since when insulin deficiency manifests as hyperglycaemia, considerable pancreatic β-cell insufficiency has already occurred.47 Thus, the third aim of this work was to identify new markers of high IR. We selected those metabolites that presented a VIP ≥ 2 and adjusted p-value <0.05 and the most predictive metabolites for high IR were chosen. The combination of DGs, uric acid and adrenic acid provided a good predictive model of high IR (AUC 80.1%). This multimetabolite biomarker model could be a comprehensive indicator of metabolic alterations before β-cell impairment occurs, as it mirrors IR in insulin-responsive tissues, lipotoxicity and certain degree of inflammation (DG), oxidative stress and alterations in carbohydrate and lipid metabolism (uric acid),30,31 and proinflammatory processes (adrenic acid).46 Further research with larger cohorts and longitudinal studies should be conducted to validate this model as an early marker of diabetes.

Strengths and Limitations

Although this study is an observational study, the high potential of untargeted metabolomics has provided a snapshot of the metabolome of subjects with high IR and/or obesity at a given time. Thus, we have explored in depth the metabolic profiles of these two metabolic disorders, described their similarities and divergences, formulated hypotheses about discordant phenotypes and mechanistic

insights, and defined a predictive model for the risk of developing diabetes. Despite the low number of subjects enrolled in the study and the fact that some individuals were grouped in both high IR and obesity groups, results were robust and in line with previously reported. Complementary metabolomics studies are necessary to provide a comprehensive overview of the metabolome of these metabolic disorders. The authors support large-scale and follow-up studies to replicate and validate the results.

CONCLUSION

Through an untargeted metabolomic-driven approach, we have explored the metabolic profiles of concordant and discordant phenotypes of subjects high IR and/or obesity. Large alterations in lipid metabolism, oxidative stress, and inflamma- tion were unveiled. In addition, these results allowed to build a multimetabolite biomarker model to predict high IR regardless of obesity that includes the measurement of DGs, uric acid, and adrenic acid. It might be also employed to predict the risk of developing diabetes; however, they need to be externally validated. These findings provide new insights in the research of metabolic diseases and unveil new potential targets in therapeutic treatments of diabetes and obesity.

ASSOCIATED CONTENT

*S Supporting Information

The Supporting Information is available free of charge on the ACS Publications website at DOI: 10.1021/acs.jproteome.7b00855. Principal component analysis score plot of quality controls and serum samples; plot correlating ions with VIP $\geq$ 2 in high IR and obesity groups in both ionization modes; variation in retention time, peak area, peak height, and detection mass in quality controls and internal and external standard samples; preprocessing parameters in MarkerView; summary of parameters for assessing OSC-PLS-DA predictive ability; summary of parameters to validate OSC-PLS-DA predictive ability; statistical significance of metabolites between phenotypic groups; ROC

curve parameters of multimetabolite biomarkers to build predictive biomarker models for high IR (PDF)

AUTHOR INFORMATION

Corresponding Author

*E-mail: candres@ub.edu. Phone: (+34) 934034840. Fax: (+34) 934035931.

ORCID

Cristina Andres-Lacueva: 0000-0002-8494-4978

Notes

The authors declare no competing financial interest. The mass spectrometry data have been deposited to the MetaboLights repository14 (https://www.ebi.ac.uk/ metabolights/) with the data set identifier MTBLS668.

ACKNOWLEDGMENTS

The authors acknowledge AB Sciex for the usage of equipment at the Warrington core facility (UK) and software programs. The authors also thank Arantxa Chicharro (former member of the University of Barcelona) for her previous work on data preprocessing. This research was supported by Project No. PI13/01172 (Plan N de I+D+i 2013−2016), cofunded by ISCII-Subdirección General de Evaluación y Fomento de la Investigación; Project No. PI-0557−2013, cofunded by Fundación Progreso y Salud, Consejería de Salud y Bienestar Social, Junta de Andaluciá , CIBERfes and CIBERobn, cofunded by Fondo Europeo de Desarrollo Regional (FEDER). 2017 SGR 1546 award from Generalitat de Catalunya's Agency AGAUR. A.M.-R., S.T., and R.G.-D. acknowledge the Juan de la Cierva postdoctoral fellowship (MINECO) and M.P.-R. the APIF fellowship (University of Barcelona).

ABBREVIATIONS

AUC, area under the curve; BCAA, branched-chain amino acids; BMI, body mass index; CI, confidence interval; DG, diglyceride; diHETE, dihydroxyeicosatetraenoic acid; ESI, electrospray ionization; FDR, false discovery rate; FFA, free fatty acids; FG, fasting glucose; GABA, γ-aminobutyric acid; HDL, high-density lipoprotein; HETE, hydroxyeicosatetraenoic acid; HOMA-IR, homeostatic model assessment−insulin resistance; IR, insulin resistance; LASSO, least absolute shrinkage and selection operator; LC−MS, liquid chromatography mass spectrometry; LDL, low-density lipoprotein; OSCPLS- DA, orthogonal signal correction partial least-squares discriminant analysis; PUFA, polyunsaturated fatty acids; QC, quality control; ROC, receiver operating characteristic; tDG, total diglycerides; TG, triglyceride; triHETE, trihydroxyeicosatetraenoic acid; VIP, variable importance in projection

REFERENCES

(1) Singh, B.; Saxena, A. Surrogate Markers of Insulin Resistance: A Review. World J. Diabetes 2010, 1 (2), 36.

(2) Lecube, A.; Monereo, S.; Rubio, M. Á.; Martínez-de-Icaya, P.; Martí, A.; Salvador, J.; Masmiquel, L.; Goday, A.; Bellido, D.; Lurbe, E.; et al. Prevention, Diagnosis, and Treatment of Obesity. 2016 Position Statement of the Spanish Society for the Study of Obesity. Endocrinol. Diabetes y Nutr. 2017, 64, 15−22.

(3) Chen, H.-H.; Tseng, Y. J.; Wang, S.-Y.; Tsai, Y.-S.; Chang, C.-S.; Kuo, T.-C.; Yao, W.-J.; Shieh, C.-C.; Wu, C.-H.; Kuo, P.-H. The Metabolome Profiling and Pathway Analysis in Metabolic Healthy and Abnormal Obesity. Int. J. Obes. 2015, 39 (8), 1241−1248.

(4) Taylor, R.; Holman, R. R. Normal Weight Individuals Who Develop Type 2 Diabetes: The Personal Fat Threshold. Clin. Sci. 2015, 128 (7), 405−410.

(5) Tulipani, S.; Palau-Rodriguez, M.; Miñarro Alonso, A.; Cardona, F.; Marco-Ramell, A.; Zonja, B.; Lopez de Alda, M.; Muñoz-Garach, A.; Sanchez-Pla, A.; Tinahones, F. J.; et al. Biomarkers of

Morbid Obesity and Prediabetes by Metabolomic Profiling of Human Discordant Phenotypes. Clin. Chim. Acta 2016, 463, 53−61.

(6) Menni, C.; Zierer, J.; Valdes, A. M.; Spector, T. D. Mixing Omics: Combining Genetics and Metabolomics to Study Rheumatic Diseases. Nat. Rev. Rheumatol. 2017, 13 (3), 174−181.

(7) Wishart, D. S. Current Progress in Computational Metabolomics. Briefings Bioinf. 2007, 8 (5), 279−293.

(8) Griffin, J. L.; Nicholls, A. W. Metabolomics as a Functional Genomic Tool for Understanding Lipid Dysfunction in Diabetes, Obesity and Related Disorders. Pharmacogenomics 2006, 7 (7), 1095− 1107.

(9) Holmes, E.; Wilson, I. D.; Nicholson, J. K. Metabolic Phenotyping in Health and Disease. Cell 2008, 134 (5), 714−717.

(10) Classification and Diagnosis of Diabetes. Diabetes Care 2016, 39 (Supplement 1), S13−S22. DOI:.

(11) Mora-Cubillos, X.; Tulipani, S.; Garcia-Aloy, M.; Bulló, M.; Tinahones, F. J.; Andres-Lacueva, C. Plasma Metabolomic Biomarkers of Mixed Nuts Exposure Inversely Correlate with Severity of Metabolic Syndrome. Mol. Nutr. Food Res. 2015, 59 (12), 2480−2490.

(12) Tulipani, S.; Mora-Cubillos, X.; Jáuregui, O.; Llorach, R.; García- Fuentes, E.; Tinahones, F. J.; Andres-Lacueva, C. New and Vintage Solutions to Enhance the Plasma Metabolome Coverage by LC-ESIMS Untargeted Metabolomics: The Not-so-Simple Process of Method Performance Evaluation. Anal. Chem. 2015, 87 (5), 2639−2647.

(13) Tulipani, S.; Llorach, R.; Urpi-Sarda, M.; Andres-Lacueva, C. Comparative Analysis of Sample Preparation Methods to Handle the Complexity of the Blood Fluid Metabolome: When Less Is More. Anal. Chem. 2013, 85 (1), 341−348.

(14) Kale, N. S.; Haug, K.; Conesa, P.; Jayseelan, K.; Moreno, P.; Rocca-Serra, P.; Nainala, V. C.; Spicer, R. A.; Williams, M.; Li, X.;et al. MetaboLights: An Open-Access Database Repository for Metabolomics Data. In Current Protocols in Bioinformatics; John Wiley & Sons, Inc.: Hoboken, NJ, 2016; Vol. 53, pp 14.13.1−14.13.18.

(15) van den Berg, R. A.; Hoefsloot, H. C.; Westerhuis, J. A.; Smilde, A. K.; van der Werf, M. J. Centering, Scaling, and Transformations: Improving the Biological Information Content of Metabolomics Data. BMC Genomics 2006, 7 (1), 142.

(16) Di Guida, R.; Engel, J.; Allwood, J. W.; Weber, R. J. M.; Jones, M. R.; Sommer, U.; Viant, M. R.; Dunn, W. B. Non-Targeted UHPLC-MS Metabolomic Data Processing Methods: A Comparative Investigation of Normalisation, Missing Value Imputation, Transformation and Scaling. Metabolomics 2016, 12 (5), 93.

(17) Meunier, B.; Dumas, E.; Piec, I.; Béchet, D.; Hébraud, M.; Hocquette, J.-F. Assessment of Hierarchical Clustering Methodologies for Proteomic Data Mining. J. Proteome Res. 2007, 6 (1), 358−366.

(18) Jourdan, F.; Breitling, R.; Barrett, M. P.; Gilbert, D. MetaNetter: Inference and Visualization of High-Resolution Metabolomic Networks. Bioinformatics 2008, 24 (1), 143−145.

(19) Fernández-Albert, F.; Llorach, R.; Andrés-Lacueva, C.; Perera, A. An R Package to Analyse LC/MS Metabolomic Data: MAIT (Metabolite Automatic Identification Toolkit). Bioinformatics 2014, 30 (13), 1937−1939.

(20) González-Dominguez, R.; García-Barrera, T.; Gómez-Ariza, J.-L. Iberian Ham Typification by Direct Infusion Electrospray and Photospray Ionization Mass Spectrometry Fingerprinting. Rapid Commun. Mass Spectrom. 2012, 26 (7), 835−844.

(21) Kim, H.-Y. Statistical Notes for Clinical Researchers: Chi- Squared Test and Fisher's Exact Test. Restor. Dent. Endod. 2017, 42 (2), 152−155.

(22) Benjamini, Y.; Hochberg, Y. Controlling the False Discovery Rate: A Practical and Powerful Approach to Multiple Testing. Journal of the Royal Statistical Society. Series B (Methodological); Wiley Royal Statistical Society, 1995; pp 289−300.

(23) Barupal, D. K.; Fiehn, O. Chemical Similarity Enrichment Analysis (ChemRICH) as Alternative to Biochemical Pathway Mapping for Metabolomic Datasets. Sci. Rep. 2017, 7 (1), 14567.

(24) Tibshirani, R. Regression Shrinkage and Selection via the Lasso. J. R. Stat. Soc. Ser. B 1996, 58, 267−288.

(25) Sumner, L. W.; Amberg, A.; Barrett, D.; Beale, M. H.; Beger, R.; Daykin, C. A.; Fan, T. W.-M.; Fiehn, O.; Goodacre, R.; Griffin, J. L.; et al. Proposed Minimum Reporting Standards for Chemical Analysis. Metabolomics 2007, 3 (3), 211−221.

(26) Erion, D. M.; Shulman, G. I. Diacylglycerol-Mediated Insulin Resistance. Nat. Med. 2010, 16 (4), 400−402.

(27) Samuel, V. T.; Petersen, K. F.; Shulman, G. I. Lipid-Induced Insulin Resistance: Unravelling the Mechanism. Lancet 2010, 375 (9733), 2267−2277.

(28) Iyer, A.; Fairlie, D. P.; Prins, J. B.; Hammock, B. D.; Brown, L. Inflammatory Lipid Mediators in Adipocyte Function and Obesity. Nat. Rev. Endocrinol. 2010, 6 (2), 71−82.

(29) Johnson, A. R.; Milner, J. J.; Makowski, L. The Inflammation Highway: Metabolism Accelerates Inflammatory Traffic in Obesity. Immunol. Rev. 2012, 249 (1), 218−238.

(30) Kodama, S.; Saito, K.; Yachi, Y.; Asumi, M.; Sugawara, A.; Totsuka, K.; Saito, A.; Sone, H. Association Between Serum Uric Acid and Development of Type 2 Diabetes. Diabetes Care 2009, 32 (9), 1737−1742.

(31) Kanbay, M.; Jensen, T.; Solak, Y.; Le, M.; Roncal-Jimenez, C.; Rivard, C.; Lanaspa, M. A.; Nakagawa, T.; Johnson, R. J. Uric Acid in Metabolic Syndrome: From an Innocent Bystander to a Central Player. Eur. J. Intern. Med. 2016, 29, 3−8.

(32) Sousa, A. G. P.; Cabral, J. V.; El-Feghaly, W. B.; de Sousa, L. S.; Nunes, A. B. Hyporeninemic Hypoaldosteronism and Diabetes Mellitus: Pathophysiology Assumptions, Clinical Aspects and Implications for Management. World J. Diabetes 2016, 7 (5), 101−111.

(33) Fox, C. S.; Larson, M. G.; Leip, E. P.; Meigs, J. B.; Wilson, P. W. F.; Levy, D. Glycemic Status and Development of Kidney Disease: The Framingham Heart Study. Diabetes Care 2005, 28 (10), 2436−2440.

(34) Ferderbar, S.; Pereira, E. C.; Apolinário, E.; Bertolami, M. C.; Faludi, A.; Monte, O.; Calliari, L. E.; Sales, J. E.; Gagliardi, A. R.; Xavier, H. T.; et al. Cholesterol Oxides as Biomarkers of Oxidative Stress in Type 1 and Type 2 Diabetes Mellitus. Diabetes/Metab. Res. Rev. 2007, 23 (1), 35−42.

(35) Bondia-Pons, I.; Ryan, L.; Martinez, J. A. Oxidative Stress and Inflammation Interactions in Human Obesity. J. Physiol. Biochem. 2012, 68 (4), 701−711.

(36) Boden, G. Obesity, Insulin Resistance and Free Fatty Acids. Curr. Opin. Endocrinol., Diabetes Obes. 2011, 18 (2), 139−143.

(37) Karpe, F.; Dickmann, J. R.; Frayn, K. N. Fatty Acids, Obesity, and Insulin Resistance: Time for a Reevaluation. Diabetes 2011, 60 (10), 2441−2449.

(38) Soga, T.; Sugimoto, M.; Honma, M.; Mori, M.; Igarashi, K.; Kashikura, K.; Ikeda, S.; Hirayama, A.; Yamamoto, T.; Yoshida, H.; et al. Serum Metabolomics Reveals γ-Glutamyl Dipeptides as Biomarkers for Discrimination among Different Forms of Liver Disease. J. Hepatol. 2011, 55 (4), 896−905.

(39) Delgado, T. C. Glutamate and GABA in Appetite Regulation. Front. Endocrinol. (Lausanne, Switz.) 2013, 4, 103.

(40) Kramer, A.; Green, J.; Pollard, J.; Tugendreich, S. Causal Analysis Approaches in Ingenuity Pathway Analysis. Bioinformatics 2014, 30 (4), 523−530.

(41) Ma, H.; Patti, M. E. Bile Acids, Obesity, and the Metabolic Syndrome. Best Pract. Res. Clin. Gastroenterol 2014, 28 (4), 573−583.

(42) Palau-Rodriguez, M.; Tulipani, S.; Isabel Queipo-Ortuño, M.; Urpi-Sarda, M.; Tinahones, F.; Andres-Lacueva, C. Metabolomic Insights into the Intricate Gut Microbial-Host Interaction in the Development of Obesity and Type 2 Diabetes. Front. Microbiol. 2015, 6, 1151.

(43) Tulipani, S.; Griffin, J.; Palau-Rodriguez, M.; Mora-Cubillos, X.; Bernal-Lopez, R. M.; Tinahones, F. J.; Corkey, B. E.; Andres-Lacueva, C. Metabolomics-Guided Insights on Bariatric Surgery versus Behavioral Interventions for Weight Loss. Obesity 2016, 24 (12), 2451−2466.

(44) Barbarroja, N.; López-Pedrera, R.; Mayas, M. D.; García- Fuentes, E.; Garrido-Sánchez, L.; Macías-González, M.; El Bekay, R.; Vidal-Puig, A.; Tinahones, F. J. The Obese Healthy Paradox: Is Inflammation the Answer? Biochem. J. 2010, 430 (1), 141−149.

(45) Moreno-Indias, I.; Oliva-Olivera, W.; Omiste, A.; Castellano- Castillo, D.; Lhamyani, S.; Camargo, A.; Tinahones, F. J. Adipose Tissue Infiltration in Normal-Weight Subjects and Its Impact on Metabolic Function. Transl. Res. 2016, 172, 6−17.e3.

(46) Nababan, S.; Nishiumi, S.; Kawano, Y.; Kobayashi, T.; Yoshida, M.; Azuma, T. Adrenic Acid as an Inflammation Enhancer in Non- Alcoholic Fatty Liver Disease. Arch. Biochem. Biophys. 2017, 623-624, 64.

(47) Wang, T. J.; Larson, M. G.; Vasan, R. S.; Cheng, S.; Rhee, E. P.; McCabe, E.; Lewis, G. D.; Fox, C. S.; Jacques, P. F.; Fernandez, C.; et al. Metabolite Profiles and the Risk of Developing Diabetes. Nat. Med. 2011, 17 (4), 448−453.

FIGURES

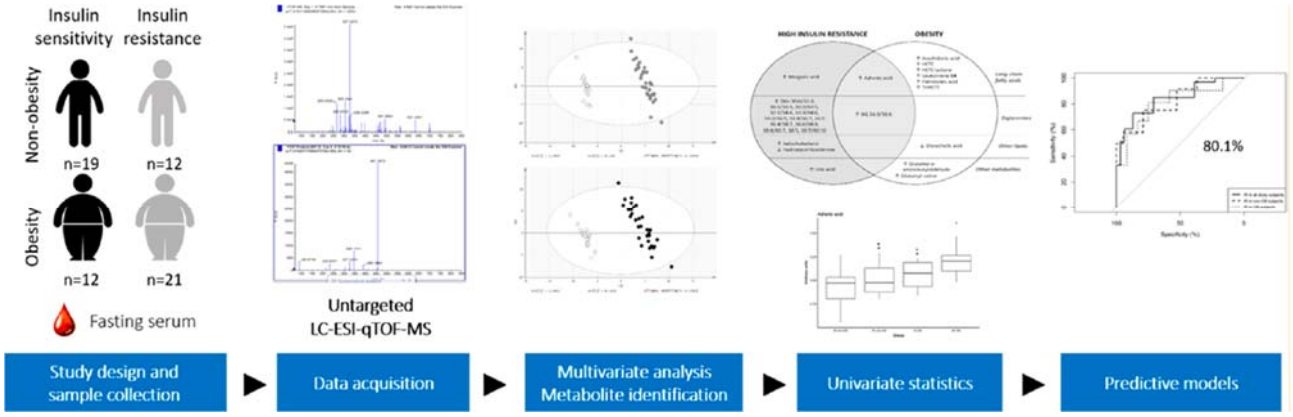

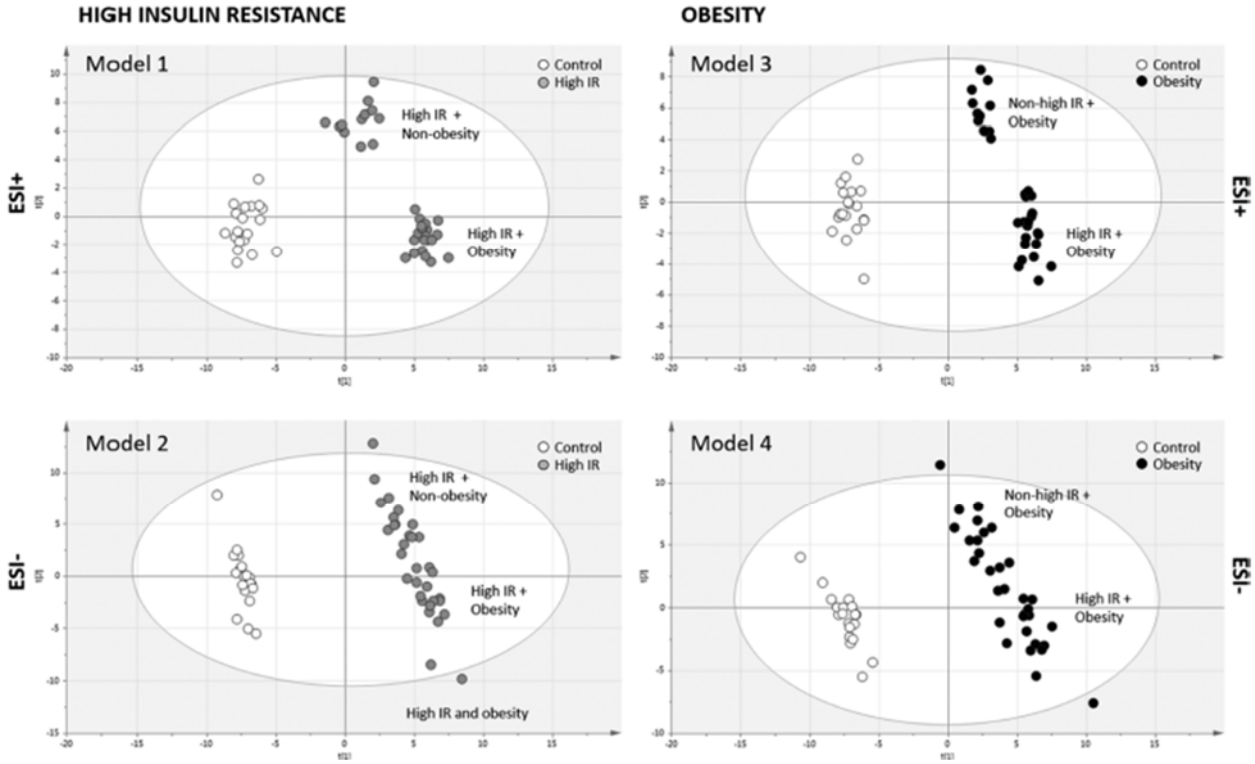

Figure 1. OSC-PLS-DA score plots. The discriminant models separated the control group (individuals with both IS and non-obesity) from patients with high IR (models 1 and 2) or subjects with obesity (models 3 and 4) in both ionization modes. White circles refer to the control group (nonobese IS), gray circles to high IR, and black circles to obesity. Abbreviations: ESI, electrospray ionization; IR, insulin resistance; IS, insulin sensitivity; OSC-PLS-DA, orthogonal signal correction partial least-squares discriminant analysis.

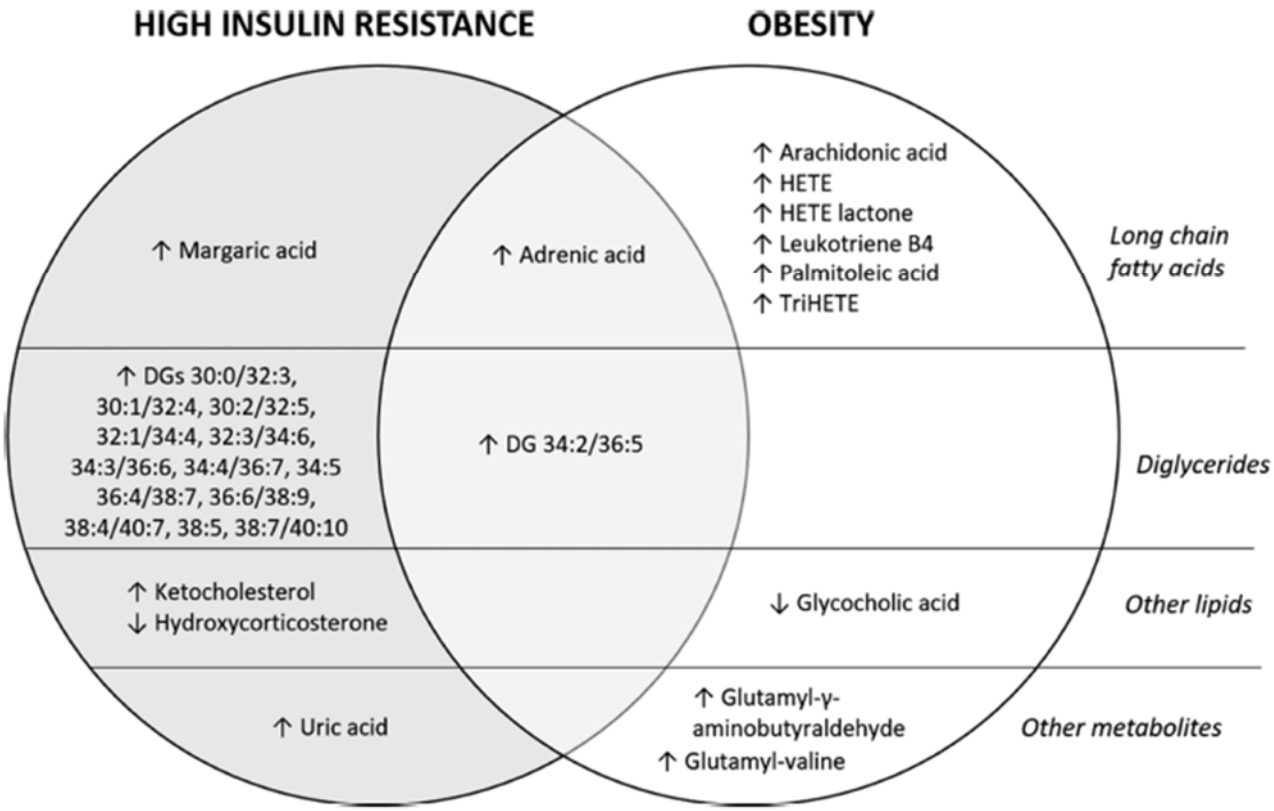

Figure 2. Venn diagram of the metabolic profiles of subjects with high IR and/or obesity. This diagram shows similarities and divergences between the metabolic status of high IR and obesity with respect to subjects with IS and non-obesity. Only metabolites that met the criteria VIP ≥ 2 and adjusted p-value ≤0.05 are shown. The symbol "/" means ambiguity in metabolite annotation.

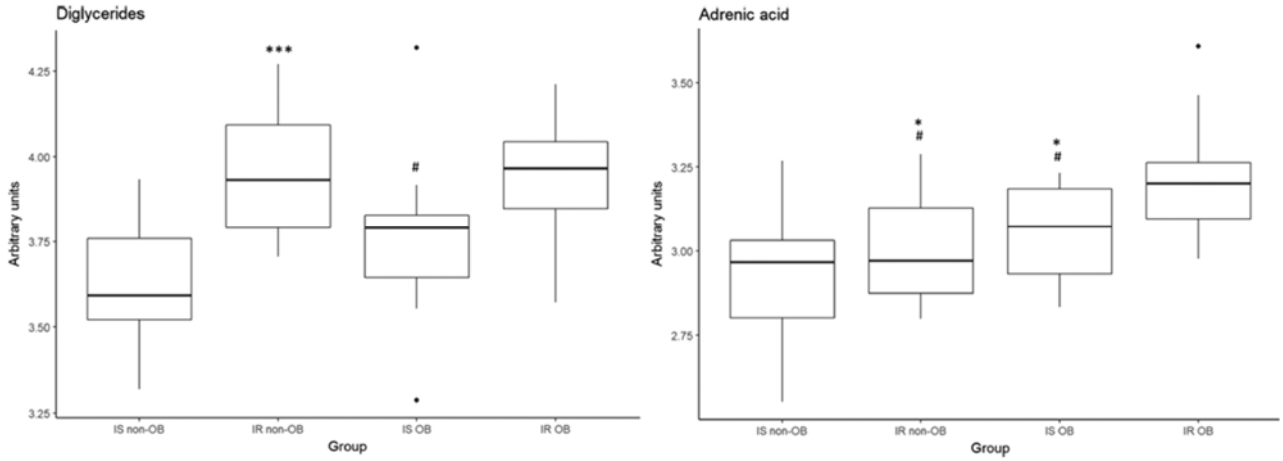

Figure 3. Box plots of the most representative metabolite changes in concordant/discordant phenotypes of high IR and obesity (Table S5). Significances (p-values) are shown with asterisks when compared with the control group as follows: ∗ $p < 0.05$, ∗∗ $p < 0.01$, ∗∗∗ $p < 0.001$; or with hash keys when compared with the group of subjects with high IR and obesity as follows: # $p < 0.05$, ## $p < 0.01$, ### $p < 0.001$. Abbreviations: IR, insulin resistance; IS, insulin sensitivity; OB, obesity.

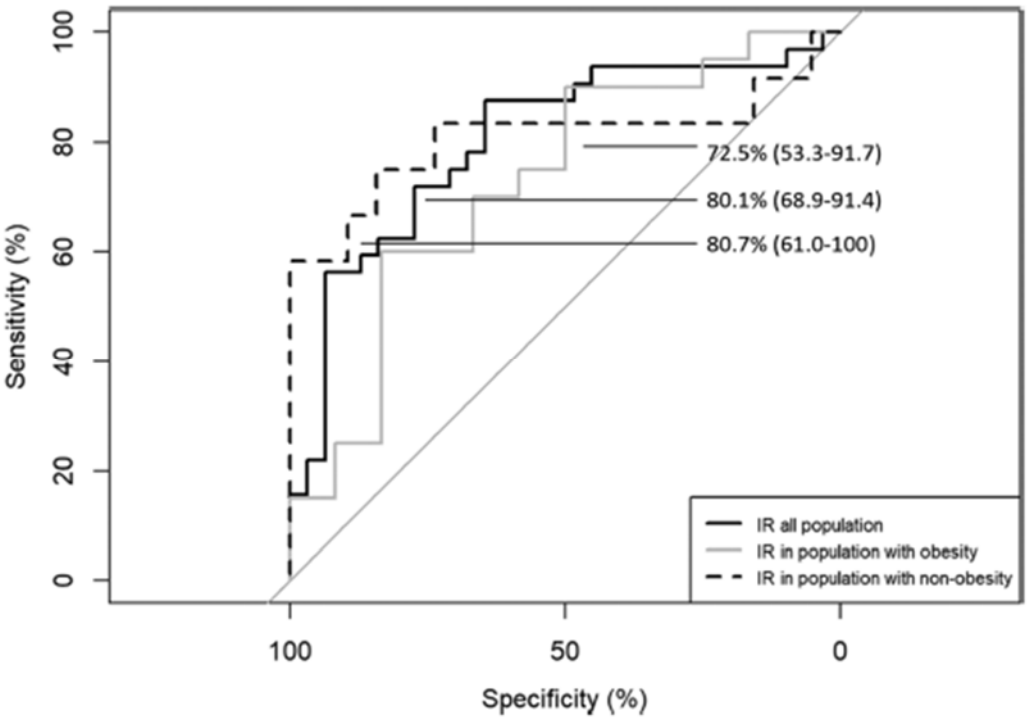

588

589 **Figure 4.** ROC curve parameters of a predictive biomarker model to identify high IR, regardless of
590 obesity. The biomarker model was formed by the arithmetic mean of the 15 DGs annotated (tDG),
591 adrenic acid, and uric acid.

592

TABLES

Table 1. Anthropometric and Biochemical Parameters of the Population of Study

	Mean ± standard deviation				P-value						
	Non-OB IS	Non-OB IR	OB IS	OB IR	IR	Obesity	IR x OB	IS: non-OB vs OB	IR: non-OB vs OB	Non-OB: IS vs IR	OB: IS vs IR
Gender	4M, 15F	4M, 8F	2M, 10F	9M, 12F	n.s.	n.s.	n.s.	n.s	n.s.	n.s.	n.s.
Age (years)	47 ± 15	53.67 ± 14.13	43.67 ± 11.30	43.14 ± 8.91	n.s.	n.s.	n.s.	n.s.	n.s.	n.s.	n.s.
Weight (kg)	64.79 ± 8.90	65.33 ± 6.58	125.77 ± 15.28	147.04 ± 30.41	n.s.	5.02E-23	n.s.	1.87E-13	3.53E-09	n.s.	n.s.
BMI (kg/m^2)	24.13 ± 1.82	24.87 ± 1.75	45.78 ± 4.67	52.67 ± 10.20	0.031	1.35E-24	n.s.	2.31E-15	3.39E-09	n.s.	n.s.
Waist circumference (cm)	82.37 ± 8.81	90.58 ± 7.97	125.09 ± 12.82	138.82 ± 14.96	0.021	3.64E-20	n.s.	5.32E-10	3.39E-08	n.s.	n.s.
Hip circumference (cm)	93.84 ± 9.97	99 ± 5.29	139.54 ± 15.56	146.56 ± 15.56	n.s.	5.60E-16	n.s.	6.44E-08	1.68E-07	n.s.	n.s.
Fasting glucose (mmol/L)	90.42 ± 7.79	111.33 ± 11.15	89.75 ± 5.58	113.95 ± 12.62	4.33E-11	n.s.	n.s.	n.s.	n.s.	1.58E-04	2.57E-06
Fasting insulin (µU/mL)	5.47 ± 2.27	14.87 ± 7.29	7.92 ± 2.36	23.89 ± 8.15	2.59E-10	n.s.	n.s.	n.s.	0.005	7.53E-04	8.81E-08
HOMA-IR (index)	1.22 ± 0.52	4.02 ± 1.82	1.76 ± 0.55	6.77 ± 2.58	1.08E-12	0.001	n.s.	n.s.	0.006	1.03E-04	1.99E-08
Systolic pressure (mm Hg)	114 ± 15	126 ± 20	142 ± 18	134 ± 17	n.s	0.001	n.s.	0.010	n.s.	n.s.	n.s.
Diastolic pressure (mm Hg)	69 ± 11	78 ± 11	88 ± 9	81 ± 8	n.s.	6.37E-04	n.s.	0.018	n.s.	n.s.	n.s.
Total cholesterol (mmol/L)	177.63 ± 23.76	232.58 ± 39.81	191.5 ± 46.38	198.90 ± 35.74	0.008	0.001	n.s.	n.s.	0.038	0.002	n.s.
HDL-cholesterol (mmol/L)	56.89 ± 10.42	52.08 ± 17.59	52.75 ± 15.52	41.5 ± 10.50	0.042	n.s.	n.s.	n.s.	n.s.	n.s.	n.s.
LDL-cholesterol (mmol/L)	103.29 ± 23.21	148.53 ± 41.17	98.04 ± 51.85	128.58 ± 29.84	0.003	n.s.	n.s.	n.s.	n.s.	0.003	n.s.
Triglycerides (mmol/L)	80.68 ± 36.46	190.75 ± 106.09	115.25 ± 107.87	149.14 ± 44.65	3.21E-04	n.s.	n.s.	n.s.	n.s.	0.002	n.s.

[a]Data are presented as mean ± standard deviation. *P*-values are based on lineal models with gender, age, and drugs as confounders. Gender distribution was explored by Fisher's exact test. *P*-values were adjusted by false discovery rate (FDR). Abbreviations: F, female; IR, insulin resistance; IS, insulin sensitivity; M, male; OB, obesity; n.s., not significant ($p > 0.05$).

Table 2. Annotated Metabolites Associated with High Insulin Resistance and Obesity[a]

Cluster[a]	Ion mode[b]	RT (min)	Detected mass[c] (m/z)	Error (mDa)	Assignation	Potential marker	Fold change[d]		P-value[e]		Level of evidence[f]
							High IR	Obesity	High IR	Obesity	
Organic acids											
1	ESI+	0.80	169.0351	0.5	[M+H]+	Uric acid	1.48	-	0.002	-	1
	ESI-	0.78	167.0209	0.2	[M-H]-						
Fatty acids											
2	ESI+	5.78	365.2063	0.0	[M+2Na-H]+	Hydroxyeicosatetraenoic acid (HETE)	4.54	4.89	n.s.	0.005	2
			343.2237	0.7	[M+Na]+						
	ESI-	5.73	523.1856	-4.5	3x[M+CHOONa]-						
			388.2153	3.3	13C[M+CHOONa]-						
			387.2136	1.7	[M+CHOONa]-						
			320.2283	2.9	13C[M-H]-						
			319.2270	0.9	[M-H]-						
			301.2166	0.2	[M-H2O-H]-						
3	ESI-	6.68	269.2471	1.5	[M-H]-	Margaric acid	1.51	-	0.045	-	1
4	ESI+	6.76	377.2423	0.4	[M+2Na-H]+	Adrenic acid	1.58	1.64	0.001	3.34E-04	1
			355.2621	-1.4	[M+Na]+						
	ESI-	6.72	399.2495	2.2	[M+CHOONa]-						
			332.2660	1.6	13C[M-H]-						
			331.2630	1.2	[M-H]-						
5	ESI+	5.77	325.2139	-0.1	[M+Na]+	Hydroxyeicosatetraenoic acid (HETE) lactone	4.98	61.43	n.s.	0.012	2
			303.2317	0.1	[M+H]+						
6	ESI-	5.35	404.2109	2.6	13C[M+CHOONa]-	Leukotriene B4 (diHETE)	63.58	66.28	n.s.	0.018	1
			403.2083	1.9	[M+CHOONa]-						
			335.2217	1.1	[M-H]-						
7	ESI+	6.29	277.2083	5.5	[M+Na]+	Palmitoleic acid	-	1.59	-	2.73E-05	1
			255.2311	0.7	[M+H]+						
			238.2243	0.3	13C[M-H-H2O]+						
			237.2208	1.0	[M-H2O+H]+						
			219.2103	1.5	[M-2H2O+H]+						
	ESI-	6.24	253.2176	-0.3	[M-H]-						
8	ESI+	6.42	328.2322	0.6	13C[M+Na]+	Arachidonic acid	-	1.58	-	0.001	1
			327.2287	0.7	[M+Na]+						
	ESI-	6.36	304.2352	1.1	13C[M-H]-						
			303.2325	0.4	[M-H]-						
9	ESI+	5.25	375.2147	-0.5	[M+Na]+	Trihydroxyeicosatetraenoic acid (triHETE)	-	6.02	-	0.009	2
Diglycerides											
10	ESI+	8.55	617.5023	0.3 or 2.7	2x13C[M+Na/H]+	Diglyceride 34:2/36:5	2.43	2.21	3.97E-06	0.022	2
			616.4992	0.1 or 2.5	13C[M+Na/H]+						
			615.4956	0.3 or 2.7	[M+Na/H]+						
11	ESI+	8.27	615.4864	0.6 or 3.0	2x13C[M+Na/H]+	Diglyceride 34:3/36:6	2.44	2.21	1.29E-05	n.s.	2
			614.4852	-1.6 or 0.8	13C[M+Na/H]+						
			613.4820	0.4 or -1.2	[M+Na/H]+						
12	ESI+	8.01	586.4528	0.5 or 1.9	13C[M+Na/H]+	Diglyceride 32:3/34:6	2.12	1.75	0.012	n.s.	2
			585.4499	-1.0 or 1.5	[M+Na/H]+						
13	ESI+	8.17	612.4683	-0.4 or 2.1	13C[M+Na/H]+	Diglyceride 34:4/36:7	2.79	2.37	4.15E-05	n.s.	2
			611.4648	-0.2 or 2.2	[M+Na/H]+						
14	ESI+	8.05	635.4653	-0.7 or 1.7	[M+Na/H]+	Diglyceride 36:6/38:9	2.83	-	4.75E-04	-	2
15	ESI+	8.01	609.4484	0.5	[M+Na]+	Diglyceride 34:5	2.64	2.25	3.69E-04	n.s.	2
16	ESI+	8.92	645.5354	-0.9	2x13C[M+H]+	Diglyceride 38:5	2.03	-	4.95E-05	-	2
			644.5326	-0.4	13C[M+H]+						
			643.5292	-2.0	[M+H]+						
17	ESI+	8.19	588.4690	-1.1 or 1.4	13C[M+Na/H]+	Diglyceride 32:2/34:5	2.21	-	3.42E-04	-	2
			587.4655	-0.9 or 1.5	[M+Na/H]+						
18	ESI+	8.18	662.4834	0.2 or 0.2	13C[M+Na/H]+	Diglyceride 38:7/40:10	2.09	-	0.004	-	2
			661.4814	-1.2 or 1.3	[M+Na/H]+						
19	ESI+	8.44	590.4844	-0.8 or 1.6	13C[M+Na/H]+	Diglyceride 32:1/34:4	2.04	-	1.50E-04	-	2
			589.4814	-1.2 or 1.3	[M+Na/H]+						
20	ESI+	8.79	668.5306	-0.1 or 2.4	13C[M+Na/H]+	Diglyceride 38:4/40:7	1.83	-	0.001	-	2
			667.5285	-1.3 or 1.1	[M+Na/H]+						
21	ESI+	8.41	641.5020	0.6 or 3.0	2x13C[M+Na/H]+	Diglyceride 36:4/38:7	1.83	-	4.97E-04	-	2
			640.4991	0.2 or 2.6	13C[M+Na/H]+						
			639.4962	-0.3 or 2.1	[M+Na/H]+						
22	ESI+	7.91	559.4338	-0.5 or 1.9	[M+Na/H]+	Diglyceride 30:2/32:5	1.58	-	0.009	-	2
23	ESI+	8.36	563.4634	1.2 or 3.6	[M+Na/H]+	Diglyceride 30:0/32:3	1.95	-	0.008	-	2
24	ESI+	8.10	562.4533	-1.0 or 2.4	13C[M+Na/H]+	Diglyceride 30:1/32:4	2.03	-	0.015	-	
			561.4488	0.1 or 2.6	[M+Na/H]+						
Other lipids											
25	ESI+	7.03	424.3265	0.2	13C[M+Na]+	Ketocholesterol, 7-	5.97	5.29	0.002	n.s.	1
			423.3235	-0.2	[M+Na]+						
			402.3444	0.4	13C[M+H]+						
			401.3413	0.1	[M+H]+						

Table 2. continued

Cluster[a]	Ion mode[b]	RT (min)	Detected mass[c] (m/z)	Error (mDa)	Assignation	Potential marker	Fold change[d]		P-value[e]		Level of evidence[f]
							High IR	Obesity	High IR	Obesity	
26	ESI+	4.82	363.2163	0.3	[M+H]+	Hydroxycorticosterone	0.62	-	0.003	-	2
27	ESI-	5.25	446.2893	1.3	[M-H2O-H]-	Glycocholic acid	-	0.51	-	1.90E-04	1
Dipeptides											
28	ESI+	3.91	284.0794	-2.5	[M+K]+	Glutamyl-Valine	-	61.43	-	0.038	2
			268.1055	-2.5	[M+Na]+						
			247.1265	-2.1	13C[M+H]+						
			246.1236	-2.6	[M+H]+						
			228.1127	-1.7	[M-H20+H]+						
29	ESI+	6.77	217.1211	-2.9	[M+H]+	γ-Glutamyl-γ-aminobutyraldehyde	-	3.06	-	0.012	2

[a]Metabolites are sorted by their VIP value in the high IR state. Abbreviations: ESI, electrospray ionization; IR, insulin resistance; n.s., not significant (adjusted *p*-value >0.05). The symbol "/" means ambiguity in metabolite annotation. [b]Clusters are listed according to decreasing VIP value. All the mass features met the criteria VIP $\geq$ 2. [c]Type of ionization. [d]Data obtained by LC-ESI-qTOF-MS. [e]Fold-change of metabolites in the high IR and obesity groups with respect to the control group. [f]Calculated with a Student's *t* test and adjusted by false discovery rate (FDR). Data were log-normalized, Pareto scaled and then adjusted by gender, age and drug consumption. [g]According to the Metabolomics Standards Initiative.[25]

Table 3. Enrichment Analysis with ChemRICH[a]

Cluster name	Cluster size	p-value	FDR	Altered metabolites
High IR				
Diglycerides	15	2.2E-20	2.2E-20	15
Obesity				
HETEs	3	5.8E-06	1.7E-05	3
Unsaturated fatty acids	4	4.0E-04	6.0E-04	4

[a]ChemRICH utilizes structure similarity and chemical ontologies to map all known metabolites and name metabolic modules. *P*-values were calculated by applying the Kolmogorov-Smirnov test. Only the metabolites that presented VIP ≥ 2 and adjusted *p*-value ≤ 0.05 were used.

Table 4. ROC Curve Parameters of Prediction Biomarker Model To Identify Subjects with High IR[a]

Prediction	Sensitivity (%)	Specificity (%)	AUC (95% CI)
High IR in all study population	71.9	77.4	80.1% (68.9-91.4)
High IR in population with obesity	60.0	83.3	72.5% (53.3-91.7)
High IR in population without obesity	75.0	84.2	80.7% (61.0-100%)

[a]Biomarker model was formed by the arithmetic mean of the 15 DGs annotated (tDG), adrenic acid and uric acid. Abbreviations: AUC, area under the curve; CI, confidence interval; IR, high insulin resistance.